Impact of Air Exposure on the Performance of the MnO_2 Cathode in Aqueous Zn Batteries

*Min Soo Jung‡, David Hoang‡, Yiming Sui, Xiulei Ji**

AUTHOR ADDRESS

Department of Chemistry, Oregon State University, Corvallis, Oregon 97331, United States

AUTHOR INFORMATION

‡ These authors contributed equally to this work

Corresponding Author

Xiulei Ji - david.ji@oregonstate.edu

ABSTRACT

We report the electrolytic manganese dioxide cathode can exhibit an initial capacity near the theoretical capacity for two-electron transfer when the testing cells are exposed to air, much greater than the cells assembled under argon. We attribute the disparity to the mechanism: MnO_2 catalyzes O_2 reduction to form an oxygen redox mediator that mediates the complete conversion of MnO_2 to Mn^{2+} ions.

TOC GRAPHIC

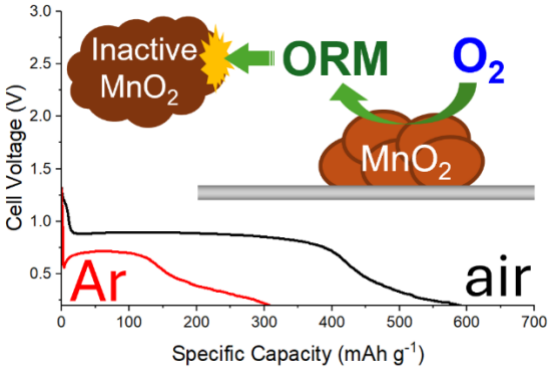

Aqueous Zn metal batteries (ZMBs) are promising to facilitate the societal shift to renewable energy by providing a sustainable and safe energy storage solution. MnO_2 stands out as the most extensively studied cathode material for ZMBs.[1] Its mechanism in acidic electrolytes can be broadly classified into: H^+ intercalation, Zn^{2+} intercalation, and Mn^{2+}(aq.) stripping,[2-5] and these processes may take place concomitantly or sequentially during discharge.[5-8] Among these mechanisms, the MnO_2/Mn^{2+} stripping/deposition process is attractive due to its theoretical capacity of 616 mAh g^{-1} for two-electron transfer. However, the full utilization of this mechanism has yet to be realized.[3,9,10] A primary challenge is the disproportionation of discharge intermediate species, *i.e.*, MnOOH, which results in the precipitation of inactive MnO_2. To address this, some reports proposed to use a redox mediator, which has shown promising progress.[7, 11] Herein, we report that air exposure of testing cells nearly realizes the theoretical capacity of the MnO_2 cathode and posit that an oxygen redox mediator (ORM), which is formed via the oxygen reduction reaction (ORR) on MnO_2, mediates the conversion of MnO_2 solid, either electrically wired or disconnected (inactive), to Mn^{2+}. Su *et al.* reported MnO_2's capacity increases from 164 to 202 mAh/g upon O_2 purging with a cutoff potential of 1 V.[12] The question is whether O_2 is reduced on the MnO_2 catalyst.[13] Herein, we report that O_2 is not only reduced when the cutoff potential is sufficiently low but converted to oxygen redox species that can mediate a complete MnO_2 reduction to Mn^{2+}.

We investigated electrolytic manganese dioxide (EMD) as the model MnO_2 cathode, tested in an electrolyte of 2 M $ZnSO_4$ + 0.5 M $MnSO_4$.[14] Figure 1 shows galvanostatic charge and discharge (GCD) potential profiles of the MnO_2||Zn cells assembled in either argon or air. The tests use a custom-designed airtight Swagelok cell that contains a headspace volume of 3.9 mL, where titanium mesh serves as the cathode current collector to ensure air permeability (Figure S1).

Cells assembled in air exhibit a high first discharge capacity of 590 mAh g^{-1}, near the theoretical capacity, in contrast to 310 mAh g^{-1} of cells assembled in Ar (Figure 1a). Su *et al.* and Tran *et al.* reported a much lower capacity of EMD, where a lower cutoff potential of 1.0 and 0.9 V, respectively, was too high for ORM to be generated.[12,14] Such capacity disparity is observed in 2 M $ZnSO_4$ as well (Figure S2). For the first charging, regardless of the atmosphere, cells exhibit capacities slightly more than 50% of their first discharge capacity, and the reversible capacity of these cells continuously increases in initial cycles. It takes 30 cycles for the Ar cell to reach a reversible capacity of 500 mAh g^{-1}; however, the air cell uses only 9 cycles to reach the same capacity (Figure 1b). It is worth noting that the capacity fades fast after the 50^{th} cycle regardless of the cell atmosphere and their GCD profiles of later cycles are similar (Figure S3, S4).

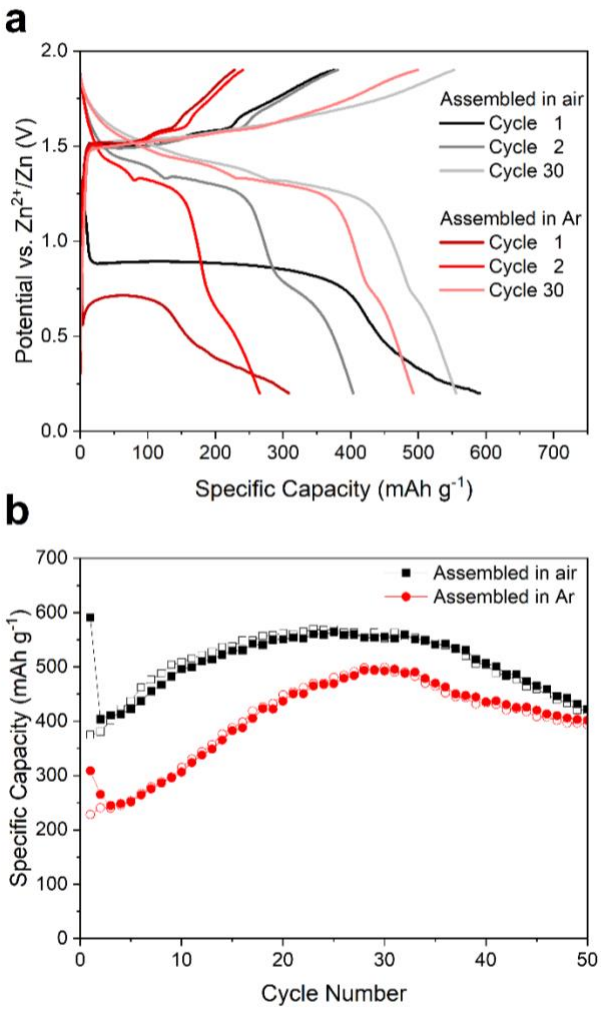

Figure 1. (a) GCD potential profiles of MnO_2||Zn cells assembled in air and Ar with the 2 M $ZnSO_4$ + 0.5 M $MnSO_4$ electrolyte. (b) Cycling performance of MnO_2||Zn cells. Hollow symbols depict charge capacity.

Cyclic voltammetry (CV) results further reveal the influence of O_2 on the EMD's performance (Figure 2a,b). In the first cathodic scan, the air cells show a more intense R1 peak near 1.1 V (vs. Zn^{2+}/Zn, and hereafter) (Figure S5), which seems to have a corresponding anodic peak of O1 at 1.6 V. O1 is known associated with the MnO_2 deposition via the direct oxidation of Mn^{2+}, supported by less intensity in an Mn^{2+}-free electrolyte (Figure S6). O1 for the air cell is much

stronger than the Ar cell, which suggests a greater concentration of Mn^{2+} in the electrolyte after the first cathodic scan under air than under argon. The higher Mn^{2+} concentration corroborates the greater initial discharge capacity of the air cell. How does air assist the more complete conversion of MnO_2 to Mn^{2+}? The answer relates to a pronounced and broad R2, peaked at 0.6 V, in the air cell, whereas R2 is absent in the Ar cell. Interestingly, R2 seems not to have a corresponding anodic peak. The more intense R1, the presence of R2 and its seemingly irreversibility, and the outsized O1 in the air cell can be best explained as such: catalytic ORR takes place as R2 (possibly R1 too), which forms an ORM; the ORM mediates the more complete conversion of MnO_2 to Mn^{2+} via a chemical reduction, thus generating more Mn^{2+} ions, responsible for the strong O1 peak. Plausible candidates for ORM are discussed in more detail in Supporting Information (SI), with a Latimer diagram (Figure S7). Regarding R1, it seems reasonable to attribute it to ORR forming peroxide (O_2/O_2^{2-}: 1.24 V, at pH=3.3); however, evidence suggests that MnO_2/Mn^{2+} stripping takes place at R1 as well. Figure S8,9 and a discussion in the SI provide a detailed rationale.

Note that the R3 and O4 peaks are assigned as electrolytic HER and OER of water, respectively. After the first cycle, R1' and R1" replace R1 regardless of the atmosphere the cells are under. These peaks may be attributed to the intercalation of Zn^{2+} or protons (R1'), followed by MnO_2/Mn^{2+} stripping (R1"). Such assignments are supported by the electrochemical quartz microbalance (EQCM) results (Figure S10), which show a mass increase during R1' and an abrupt mass loss at R1" due to the peeling-off of the deposited mass. R2 diminishes in the second cycle. One factor is that the deposited MnO_2 strips into Mn^{2+}, preventing its catalysis to generate ORM. As another factor, the deposited Zn-containing phases are not as catalytic as the pristine EMD (Figure S11).

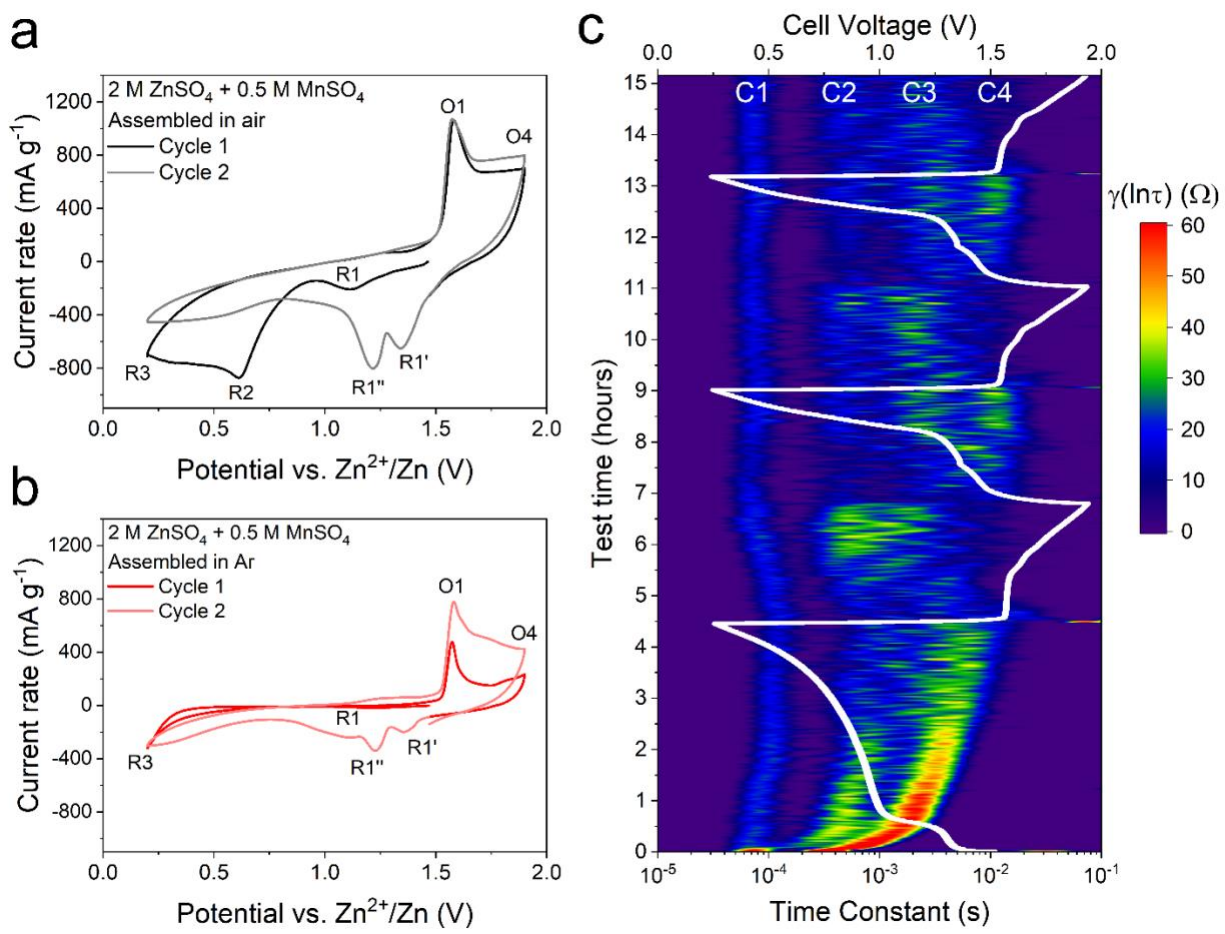

Figure 2. (a,b) Cyclic voltammograms of the MnO_2||Zn cells with the 2 M $ZnSO_4$ + 0.5 M $MnSO_4$ electrolyte under different atmospheres. (c) DRT analysis results of the operando galvano EIS data acquired during galvanostatic cycling of 3-electrode cells assembled in air.

Distribution of Relaxation Time (DRT) analysis of the operando Galvano Electrochemical Impedance Spectroscopy (GEIS) was conducted to deconvolute different charge transfer events of the electrode during the GCD cycling (Figure 2c).[15] The slowest C4 appears only during discharge, which can be attributed to ORR-related charge transfer. This assignment is also supported by C3-dominating profiles of the N_2-purged cells (Figure S9) and strong C4 peaks

during discharge below 1.2 V in O_2-purged cells (Figure S10). More DRT discussion is provided in SI.

In summary, we report the impact of air exposure by the MnO_2||Zn testing cells on their electrochemical performance. We suggest that the enhanced initial capacity of the MnO_2 cathode is due to the oxygen redox mediator that is formed via ORR. This study highlights the role of oxygen gas in testing the performance of the MnO_2 cathode.

ASSOCIATED CONTENT

Supporting Information

A schematic of a 2-electrode and a 3-electrode Swagelok cell, Electrochemical performance data of 2 M $ZnSO_4$ cells, extra CV data, EQCM experiment results, XRD patterns of cathodes, supplementary discussions, additional experimental details, and materials preparations.

AUTHOR INFORMATION

group website - https://jigroup.chem.oregonstate.edu/

Notes

The authors declare no competing financial interest."

ACKNOWLEDGMENT

X.J. thanks National Science Foundation for the financial support, Grant Numbers: DMR-2221645 and CBET-2038381.

REFERENCES

(1) Chao, D.; Zhou, W.; Ye, C.; Zhang, Q.; Chen, Y.; Gu, L.; Davey, K.; Qiao, S.-Z. An Electrolytic Zn–MnO_2 Battery for High-Voltage and Scalable Energy Storage. *Angew. Chem. Int. Ed.* **2019**, 58 (23), 7823-7828. **DOI:** 10.1002/anie.201904174

(2) Yuan, Y.; Sharpe, R.; He, K.; Li, C.; Saray, M. T.; Liu, T.; Yao, W.; Cheng, M.; Jin, H.; Wang, S.; et al. Understanding Intercalation Chemistry for Sustainable Aqueous Zinc–Manganese Dioxide Batteries. *Nat. Sustain.* **2022**, 5 (10), 890-898. **DOI:** 10.1038/s41893-022-00919-3

(3) Moon, H.; Ha, K.-H.; Park, Y.; Lee, J.; Kwon, M.-S.; Lim, J.; Lee, M.-H.; Kim, D.-H.; Choi, J. H.; Choi, J.-H.; Lee, K. T. Direct Proof of the Reversible Dissolution/Deposition of Mn^{2+}/Mn^{4+} for Mild-Acid Zn-MnO_2 Batteries with Porous Carbon Interlayers. *Adv. Sci.* **2021**, 8 (6), 2003714. **DOI:** 10.1002/advs.202003714

(4) Rodríguez-Pérez, I. A.; Chang, H. J.; Fayette, M.; Sivakumar, B. M.; Choi, D.; Li, X.; Reed, D. Mechanistic Investigation of Redox Processes in Zn–MnO_2 Battery in Mild Aqueous Electrolytes. *J. Mater. Chem. A* **2021**, 9 (36), 20766-20775. DOI: 10.1039/D1TA05022B.

(5) Sun, W.; Wang, F.; Hou, S.; Yang, C.; Fan, X.; Ma, Z.; Gao, T.; Han, F.; Hu, R.; Zhu, M.; Wang, C. Zn/MnO_2 Battery Chemistry With H^+ and Zn^{2+} Coinsertion. *J. Am. Chem. Soc.* **2017**, 139 (29), 9775-9778. **DOI:** 10.1021/jacs.7b04471

(6) Li, C.; Yuan, H.; Liu, T.; Zhang, R.; Zhu, J.; Cui, H.; Wang, Y.; Cao, D.; Wang, D.; Zhi, C. Distinguish MnO_2/Mn^{2+} Conversion/ Zn^{2+} Intercalation/ H^+ Conversion Chemistries at Different Potentials in Aqueous Zn||MnO_2 Batteries. *Angew. Chem. Int. Ed.* **2024**, 63 (22), e202403504. **DOI:** 10.1002/anie.202403504

(7) Ye, X.; Han, D.; Jiang, G.; Cui, C.; Guo, Y.; Wang, Y.; Zhang, Z.; Weng, Z.; Yang, Q.-H. Unraveling the Deposition/Dissolution Chemistry of MnO_2 for High-Energy Aqueous Batteries. *Energy Environ. Sci.* **2023**, 16 (3), 1016-1023. **DOI:** 10.1039/D3EE00018D

(8) Chen, X.; Li, W.; Zeng, Z.; Reed, D.; Li, X.; Liu, X. Engineering Stable Zn-MnO_2 Batteries by Synergistic Stabilization Between the Carbon Nanofiber Core and Birnessite-MnO_2 Nanosheets Shell. *Chem. Eng. J.* **2021**, 405, 126969. **DOI:** 10.1016/j.cej.2020.126969.

(9) Kim, S. J.; Wu, D.; Sadique, N.; Quilty, C. D.; Wu, L.; Marschilok, A. C.; Takeuchi, K. J.; Takeuchi, E. S.; Zhu, Y. Unraveling the Dissolution-Mediated Reaction Mechanism of α-MnO_2 Cathodes for Aqueous Zn-Ion Batteries. *Small* **2020**, 16 (48), 2005406. **DOI:** 10.1002/smll.202005406

(10) Xiao, X.; Zhang, Z.; Wu, Y.; Xu, J.; Gao, X.; Xu, R.; Huang, W.; Ye, Y.; Oyakhire, S. T.; Zhang, P.; et al. Ultrahigh-Loading Manganese-Based Electrodes for Aqueous Batteries via Polymorph Tuning. *Adv. Mater.* **2023**, 35 (33), 2211555. **DOI:** 10.1002/adma.202211555

(11) Liu, Y.; Xie, C.; Li, X. Bromine Assisted MnO_2 Dissolution Chemistry: Toward a Hybrid Flow Battery with Energy Density of over 300 Wh L^{-1}. *Angew. Chem. Int. Ed.* **2022**, 61 (51), e202213751. **DOI:** 10.1002/anie.202213751

(12) Su, L.; Liu, L.; Liu, B.; Meng, J.; Yan, X. Revealing the Impact of Oxygen Dissolved in Electrolytes on Aqueous Zinc-Ion Batteries. iScience 2020, 23 (4). **DOI:** 10.1016/j.isci.2020.100995

(13) Worku, A. K.; Ayele, D. W.; Habtu, N. G.; Teshager, M. A.; Workineh, Z. G. Recent Progress in MnO_2-Based Oxygen Electrocatalysts for Rechargeable Zinc-Air Batteries. *Mater. Today Sustain.* **2021**, 13, 100072. **DOI:**10.1016/j.mtsust.2021.100072.

(14) Tran, T. N. T.; Jin, S.; Cuisinier, M.; Adams, B. D.; Ivey, D. G. Reaction mechanisms for electrolytic manganese dioxide in rechargeable aqueous zinc-ion batteries. *Sci. Rep.* **2021**, 11 (1), 20777. **DOI:** 10.1038/s41598-021-00148-2.

(15) Wan, T. H.; Saccoccio, M.; Chen, C.; Ciucci, F. Influence of the Discretization Methods on the Distribution of Relaxation Times Deconvolution: Implementing Radial Basis Functions with DRTtools. *Electrochim. Acta* **2015**, 184, 483-499. **DOI:** j.electacta.2015.09.097.